Journal of the Optical Society of America B
OPTICAL PHYSICS

Asymmetric light transmission based on a 1D triangular metal grating

Yu Lin

National Engineering Research Center for Diffraction Gratings Manufacturing and Application, Changchun Institute of Optics and Fine Mechanics and Physics, Chinese Academy of Sciences, Changchun, Jilin 130033, China (e-mail: linyu@ciomp.ac.cn)

Received 14 January 2020; revised 21 March 2020; accepted 21 March 2020; posted 23 March 2020 (Doc. ID 387975); published 23 April 2020

Here, we present a 1D isosceles triangle silver grating on the dielectric substrate. The grating performs asymmetric light transmission (ALT) characteristics for the light with both transverse magnetic (TM) and transverse electric (TE) polarization states over a waveband in the vicinity of 1.55 μm. By checking the efficiency of each diffraction order and the distribution of the electromagnetic field, we found that the ALT characteristics originate from the high transmitted or reflected diffraction channels excited by forward and backward direction incidence. The grating shows the ALT characteristics in a waveband where incident wavelengths are less and more than the period, so that the grating may be a candidate for the wideband ALT devices. It is worth stressing that the contrast ratio (CR) at a specific wavelength can exceed more than 29 dB (the incident angle is 5.6897°; the incident wavelength is 1.7759 μm) under oblique incidence.

https://doi.org/10.1364/JOSAB.387975

1. INTRODUCTION

Asymmetric light transmission (ALT) is also called unidirectional light transmission [1–3] or optical diode [4,5]. Light flowing through an ALT device is just like the current passing through a diode; light can be transmitted from one direction and blocked from the reverse direction. ALT devices have aroused the attention of researchers because of their extensive applications, such as source protection [6–8], optical information processing [9–11], solar energy systems [12], optical sensing [6,13], etc.

Conventional methods for realizing ALT are based on magnetic-optical materials or nonlinear materials [14,15]. However, they are challenging to integrate into small optoelectronic systems due to their ponderous and bulky shortcomings. In recent decades, with the development of the nanotechnology and micronano optics, researchers have achieved ALT by artificial structures, such as chiral structure [16–18], 2D composite gratings [9,12], subwavelength holes [19–21], photonic crystal [22,23], a slice of other metamaterials [14,24–26], and so on. Among the above works, the ALT effect originating from the diffraction asymmetry was reported by Zhu *et al.* [9]; the effect is useful to design the polarization-independent ALT devices. It is necessary to apply this effect to 1D gratings and have some insight into the diffraction asymmetry (disappearance of diffraction orders or energy conversion between different diffraction orders). Compared to the types of complex 2D or 3D artificial micronano structures mentioned above, the traditional 1D diffraction gratings allow mass production and practical application to be more easily achieved. The possibility of ALT of the 1D diffraction gratings has been verified in some previous studies [1–3,6,27–32]. Ye *et al.* [1], Xu *et al.* [3], Stolarek *et al.* [27], Qiu and Xu [29], and Xu *et al.* [32] have designed the ALT devices by combing double 1D gratings with different periods. Ba *et al.* [6] have realized ALT based on a three-layer metal grating structure. Tang *et al.* [28] and Zhu *et al.* [30] have designed the metallic grating with the dielectric substrate to make ALT devices. The gratings perform the ALT phenomenon only for transverse magnetic (TM) polarized light because they are based on unidirectional excitation of surface plasmon polaritons (SPPs) [28,30]. All of the above positive results inspired us to utilize diffraction gratings to realize ALT. However, there are still some deficiencies here. First, double gratings or multiplayer gratings increase the complexity of the device, reducing the stability of optical performance. Second, most of the ALT devices are dependent on the polarization states of the incident light, because they work by unidirectional excitation of SPPs [6,28,30]. SPPs do not exist for the TE polarization state [33], so the applications of the devices are limited. Gao *et al.* [2], Tang *et al.* [28], and Zinkiewicz *et al.* [31] have realized ALT in the visible light waveband based on a simple 1D rectangular or trapezoidal grating; their studies increase our desire to use a simple 1D triangular grating to achieve ALT over a waveband in the vicinity of 1.55 μm.

In this study, we present a 1D isosceles triangle sliver grating on the dielectric substrate. The grating performs ALT over a

waveband in the vicinity of 1.55 μm by parameter optimization. With the analysis of numerical simulation, we get that the ALT characteristics can be explained by means of the channel effect. There are different transmitted or reflected diffraction order channels under forward and backward illuminations. The grating performs ALT for the light with both the TM and the transverse electric (TE) polarization states, and it works positively in a waveband where the incident wavelengths are less and larger than the period. The high contrast ratio (CR) at a specific wavelength can be obtained under oblique incidence. The paper is organized as follows. First, a 1D grating structure and its parameter optimization are presented in Section 2. Then, the results and discussions are given in Section 3. Last, the summary is made in Section 4.

2. GRATING STRUCTURE

Figure 1 depicts the schematic view of a 1D isosceles triangle sliver grating on the semi-infinite dielectric substrate. The grating period is Λ. The base of the triangle is placed in the middle of one unit. Its length is $f\Lambda$ (f is the fill factor of the grating). The base angle of the triangle is β. The refractive indexes of the air and the dielectric substrate are $n_a = 1$, $n_s = 1.44$, respectively. The dielectric function of silver characterized by the Lorentz–Drude model can be expressed by the following equation [21,34]:

$$\varepsilon(\omega) = 1 - \frac{f_0{\omega_p}^2}{\omega(\omega - i\Gamma_0)} + \sum_{j=1}^{k} \frac{f_j{\omega_p}^2}{({\omega_j}^2 - \omega^2) + i\omega\Gamma_j}. \quad (1)$$

Here, ω_p is the plasma frequency. k is the number of oscillators with frequency ω_j. f_j is oscillator strength. Γ_j is the damping constant. The values of all parameters mentioned above in Eq. (1) can be obtained from [34].

We want to ensure that the grating is easy to be fabricated and is less sensitive to the polarization states of the incident light. The fill factor (f) should be neither too large nor too small. To simplify the design process, we set the value of the fill factor (f) to be 0.65 initially. First, we obtained the total transmittance at incident wavelength $\lambda = 1.55$ μm with different grating periods and base angles of the isosceles triangle by rigorous coupled-wave analysis (RCWA). The structure was simulated employing periodic conditions along the x axes and perfectly matched layer (PML) along the y axes. Forward and backward transmittance of TE (the electric field vector parallel to the z axis) and TM polarization (the magnetic field vector parallel to the z axis) states at 1.55 μm under the normal incidence ($\theta = 0°$) are shown in Fig. 2. As illustrated in Fig. 2, the forward transmittance is greater than the backward transmittance. We know that the simple 1D triangular metal grating shows the ALT characteristics. The backward transmittances are almost below 0.4 [Figs. 2(c) and 2(d)]. With the change of the period (Λ) and the base angle (β), their fluctuation ranges are small. The forward transmittances for both of the TE and TM lights are with high values when the period is 1.55 μm [Figs. 2(a) and 2(b)], and they increase with the base angle (β). However, the backward transmittances increase with the base angle (β) too. We want to suppress the backward transmittance and obtain the better ALT characteristics for the grating, so the grating period (Λ) and base angle (β) of the isosceles triangle are selected to be $\Lambda = 1.55$ μm, $\beta = 45°$, respectively.

Then, after obtaining the period (Λ) and the base angle (β), we calculated the total transmittance at 1.55 μm for varying the fill factor (f) under the normal incidence. We define the forward transmittance as T_F, the backward transmittance as T_B, and the transmittance difference as $T_F - T_B$. As shown

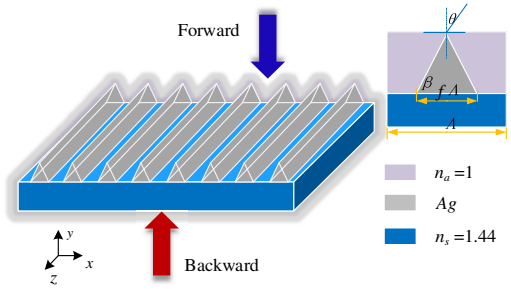

Fig. 1. Schematic view of a 1D isosceles triangle metal grating on the semi-infinite dielectric substrate. The blue and red arrows indicate forward and backward directions.

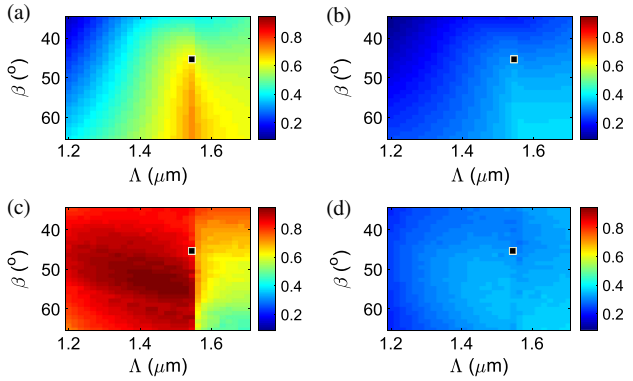

Fig. 2. Total transmittance at 1.55 μm calculated for varying the grating period (Λ) and isosceles triangle base angle (β). (a) Forward transmittance and (b) backward transmittance of TE polarization state. (c) Forward transmittance and (d) backward transmittance of TM polarization state. Where $\Lambda = 1.55$ μm, $\beta = 45°$ are marked with black dots. The results are obtained for $n_a = 1$, $n_s = 1.44$, $f = 0.65$.

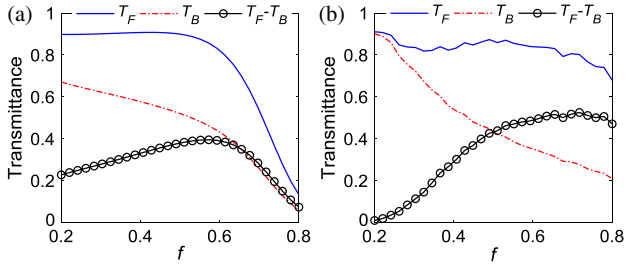

Fig. 3. Total transmittance at 1.55 μm calculated for varying the fill factor (f). Forward transmittance (blue solid line), backward transmittance (red dash-dotted line), and transmittance difference (black solid line with circles) of (a) TE and (b) TM polarization states. The results are obtained for $n_a = 1$, $n_s = 1.44$, $\Lambda = 1.55$ μm, $\beta = 45°$.

in Fig. 3, for the TE polarization state [Fig. 3(a)], the transmittance difference increases first and then decreases with the increase of the fill factor (f). The transmittance difference gets the maximum value when the fill factor (f) is 0.6. However, the backward transmittance is slightly higher at this point. As for the TM polarization state [Fig. 3(b)], with the increase of the fill factor (f), the transmittance difference first increases and then becomes flat (there is a slight downward trend here). Based on the above analysis, 0.65 is not a wrong choice for the fill factor (f) value to ensure that the grating has a significant transmittance difference for TE and TM polarization states.

3. RESULTS AND DISCUSSION

After determining the parameters of a 1D triangular metal grating, we calculated the forward and backward transmission spectra from 1 to 2.5 μm under the normal incidence. The numerical results are illustrated in Fig. 4; they show that the grating performs the ALT characteristics until about 2.23 μm. First, as shown in the inset of Fig. 4(a), for TE polarized light, the forward transmittance is 0.71 at 1.55 μm; the backward transmittance is 0.35 at 1.55 μm. Second, as shown in the inset of Fig. 4(b), for TM polarized light, the forward transmittance is 0.83 at 1.55 μm; the backward transmittance is 0.31 at 1.55 μm. At the same time, the spatial distribution of the normalized $|\mathbf{H_x}| + |\mathbf{H_z}|$ at 1.55 μm was calculated by the finite element method (FEM). We set the incident magnetic field with 1 V/m x-direction and z-direction components because the grating performs the ALT characteristics for both of the TE and TM lights. The boundary conditions are the same as Section 2. The spatial distribution of the normalized $|\mathbf{H_x}| + |\mathbf{H_z}|$ of the light at 1.55 μm illuminating from forward and backward directions are depicted as Figs. 4(c) and 4(d), respectively. The white arrows indicate the incident directions. Figs. 4(c) and 4(d) show the ALT characteristics of the structure at 1.55 μm visually; they can show ALT for both of the TE and TM lights. Light can flow through the structure under the forward illumination [Fig. 4(c)], but it is blocked by the structure under the backward illumination [Fig. 4(d)]. Transmission spectra in Figs. 4(a) and 4(b) show a clear fact that the forward transmittance is more than twice the backward transmittance for both of the TE and TM lights at 1.55 μm. Compared to TE polarized light, this grating shows a more obvious ALT phenomenon for TM polarized light in the same waveband, because TM polarized light shows higher forward transmittance than TE polarized light in the same wideband. As shown in Figs. 4(a) and 4(b), the ALT phenomenon disappears when the incident wavelengths exceed 2.23 μm. In order to further analyze and understand the ALT characteristics of this structure, we calculated forward and backward diffractive spectra of different diffraction orders under the normal incidence.

Figures 5(a) and 5(b) show the forward and backward diffractive spectra of TE polarized light; Figs. 5(c) and 5(d) show the forward and backward diffractive spectra of TM polarized light. An interesting phenomenon is shown in Fig. 5. Compared to the forward and backward incidence, the high diffraction orders (positive and negative first diffraction orders) will be switched from the transmission beams under forward incidence to the reflection beams under backward incidence. From the incident

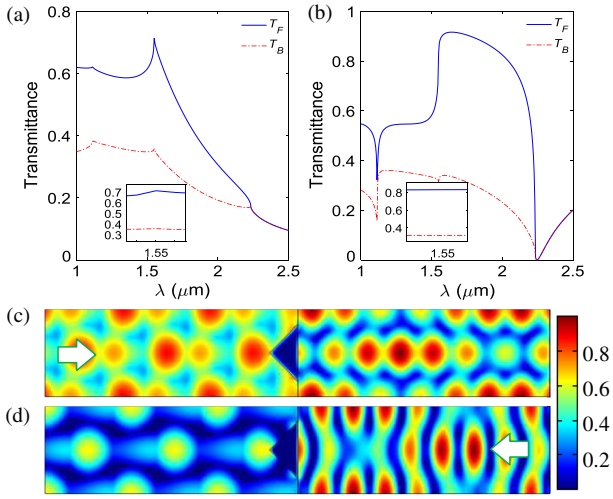

Fig. 4. Forward (blue solid line) and backward (red dash-dot line) transmittance of (a) TE and (b) TM polarization states. The insets show the transmittance at 1.55 μm. Spatial distribution of the normalized magnetic-field intensity $|\mathbf{H_x}| + |\mathbf{H_z}|$ for the incident light at 1.55 μm under (c) forward and (d) backward illuminations. The white arrows indicate the incident direction.

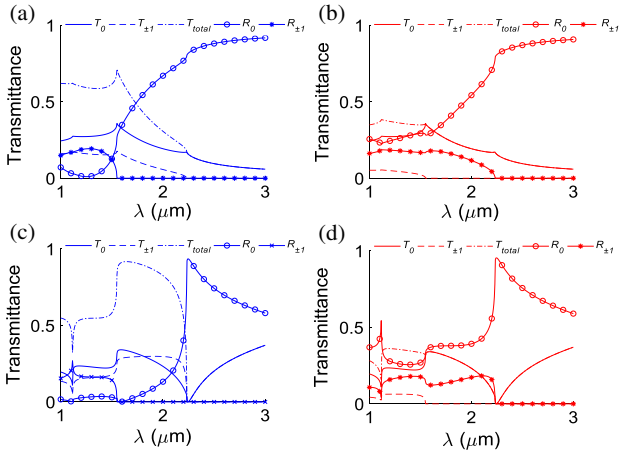

Fig. 5. Diffraction efficiency of different diffraction orders. (a) Forward and (b) backward diffraction efficiency of TE polarized light. (c) Forward and (d) backward diffraction efficiency of TM polarized light.

wavelength at 1.55 μm, the positive and negative first transmitted diffraction orders (they are with the same transmittance, because of the normal incidence and left–right symmetry of the grating) exist under the forward incidence as shown the blue-dashed lines in Figs. 5(a) and 5(c), but they disappear under the backward incidence because the positive and negative first transmitted diffraction orders switch to the positive and negative first reflected diffraction orders, as shown by the red lines with asterisks in Figs. 5(b) and 5(d). The incident wavelength is precisely equal to the period of the grating. However, the high diffraction orders disappear at 2.23 μm. Only the zeroth transmitted and reflected orders are to propagate, so the grating performs no ALT characteristics. The reciprocal theorem [2,19] is still valid in this structure. The ALT characteristics of the grating are due to the

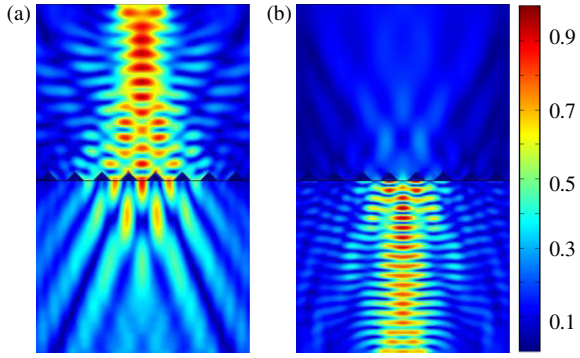

Fig. 6. Spatial distribution of the normalized magnetic-field intensity $|\mathbf{H_x}| + |\mathbf{H_z}|$ under the (a) forward and (b) backward illuminations at 1.55 μm.

difference in the energy distribution of diffraction orders under forward and backward illuminations. The high diffraction orders are transmitted under forward incidence, while the high diffraction orders are reflected under backward incidence. Why is the incident wavelength 2.23 μm when the high diffraction orders and ALT phenomenon disappear? We can get it by the following equation [35]:

$$\lambda < \Lambda[\max(n_a, n_s) + n_a \sin\theta], \tag{2}$$

where max holds for the maximum of the arguments (n_a, n_s). The parameters, including λ, Λ, n_a, n_s, and θ, are shown as Fig. 1. In this structure, we can get the cutoff value of wavelength (λ) of 2.232 μm by Eq. (2) under the normal incidence. It is in a positive argument with our numerical results (the result of the numerical calculation is about 2.23 μm). To verify the aforementioned idea and understand the ALT characteristics of the grating more intuitively, we attempted to visualize the propagation direction of the diffracted beams. The electromagnetic field distribution of the grating was obtained by the FEM again. However, different from the previous simulation, a finite width grating illuminated by light [the incident magnetic field is the same as Figs. 4(c) and 4(d)] with a limited width was analyzed. The structure was simulated employing scattering conditions along the x axes and PML along the y axes. Figure 6 depicts the distribution of normalized $|\mathbf{H_x}| + |\mathbf{H_z}|$ under forward and backward incidence. As shown in Fig. 6(a), more energies pass through the grating. The transmission lights are with different outgoing diffractive propagation directions, so the high transmitted diffraction orders exist under forward illumination. However, as depicted in Fig. 6(b), little energies pass through the grating, and they are reflected, so the high reflected diffraction orders exist under backward illumination. Combined with Figs. 5 and 6, the ALT characteristics of this structure are determined by the different energy distribution of transmitted and reflected diffraction orders when light is illuminated from the forward and backward direction.

In previous works [2,28], there are some studies based on a similar principle (the high diffraction orders are depressed under backward illumination) to design the ALT gratings. However, our structure is based on the triangles, resulting in the disappearance of high transmitted and reflected diffraction orders under forward and backward directions at different incident wavelengths, so the ALT characteristics are maintained in this waveband. Compared to the previous works based on a 1D rectangular [2] or trapezoidal grating [28], the grating we designed can keep the ALT characteristics with the more extended range, where the incident wavelengths are greater than the period. Maybe the triangular grating has excellent potential to realize wideband ALT characteristics.

Finally, we analyze the ALT characteristics of the grating under oblique incidence. The CR is computed from the definition in Eq. (3) to characterize the ALT of this structure:

$$\mathrm{CR} = 10 \log\left(\frac{T_F}{T_B}\right). \tag{3}$$

Figure 7 describes the change of total transmission spectra along with the incident angles and incident wavelengths. Figures 7(a)–7(c) show the transmittance of TE polarized light under forward incidence, backward incidence, and the CR, respectively; Figs. 7(d)–7(f) show the transmittance of TM polarized light under forward incidence, backward incidence, and the CR, respectively. With the increase of incident angle, the change of the ALT characteristics is not obvious for TE polarized light. However, it is more dependent on the incident angle and incident wavelength for TM polarized light. It is worth mentioning that the CR can exceed more than 29 dB at the specific

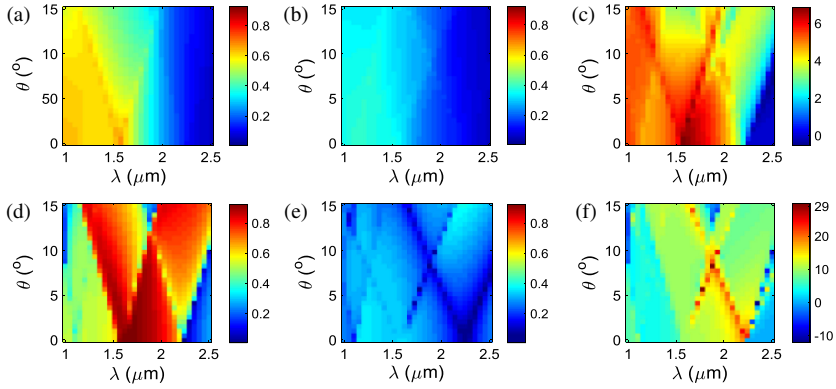

Fig. 7. Transmittance and CR of TE and TM polarized lights as functions of incident wavelength (λ) and incident angle (θ). (a) Forward transmittance, (b) backward transmittance, and (c) CR of TM polarized light. (d) Forward transmittance, (e) backward transmittance, and (f) CR of TM polarized light.

incident wavelength and incident angle [Fig. 7(f)], where the incident angle and the incident wavelength are 5.6897° and 1.7759 μm, respectively. Therefore, in practical application, the grating may bring better ALT characteristics under the oblique incidence. As for the incident wavelength at 1.55 μm, the CR is not sensitive to the incident angle θ [Figs. 7(c) and 7(f)]. Then, in combination with the total transmittance as a function of the triangle base angle β [Fig. 2], we know there is little influence on the ALT characteristics of the grating with the small error of base angle (β) machining and the error of incident angle (θ), which is beneficial to the structure application in engineering practice.

The fabrication of triangular metal gratings on the dielectric substrate is challenging. Sridharan and Bhattacharya [36] presented a method of fabricating a triangular grating in quartz. The part of steps such as electron beam lithography (EBL), metal evaporation, and lift-off in their process can guide us to fabricate the grating we designed. Fused silica can be selected as the substrate because the refractive index of fused silica is 1.444 at 1.55 μm [37]; it is approximately equal to the refractive index (1.44) in the simulation. We hope experiments in the future will support our ideas.

4. SUMMARY

In summary, we analyzed a simple 1D triangular sliver grating on the semi-infinite dielectric substrate. The high diffraction orders are transmission beams under forward illumination, but they switch from the transmission beams to the reflection beam under reversion illumination. So the grating shows the ALT phenomenon. Both of the TE and TM lights are equally effective. When the incident wavelength is 1.55 μm, the forward transmittances of the TE and TM lights are 2 and nearly 3 times that of the backward transmittances, respectively. Moreover, the ALT characteristics of the grating are effective in a waveband where the incident wavelengths are less or greater than the period. Under oblique incidence, the CR for TM polarized light can exceed more than 29 dB (the incident angle is 5.6897°; the incident wavelength is 1.7759 μm). We believe that the triangular metal gratings are a choice to achieve wideband ALT. Our idea can be extended to other wavebands. Our studies are helpful to give some insights into the ALT characteristics of the 1D triangular metal gratings. There are positive effects on studying the ALT phenomenon in our work.

Acknowledgment. The author thanks all staff of the National Engineering Research Center for Diffraction Gratings Manufacturing and Application of China.

Disclosures. The authors declare no conflicts of interest.

REFERENCES

1. W. M. Ye, X. D. Yuan, and C. Zeng, "Unidirectional transmission realized by two nonparallel gratings made of isotropic media," Opt. Lett. **36**, 2842–2844 (2011).
2. H. Gao, Z. Zheng, J. Dong, J. Feng, and J. Zhou, "Multi-frequency optical unidirectional transmission based on one-way guided mode resonance in an extremely simple dielectric grating," Opt. Commun. **355**, 137–142 (2015).
3. J. Xu, C. Cheng, M. Kang, J. Chen, Z. Zheng, Y. X. Fan, and H. T. Wang, "Unidirectional optical transmission in dual-metal gratings in the absence of anisotropic and nonlinear materials," Opt. Lett. **36**, 1905–1907 (2011).
4. C. Wang, C. Z. Zhou, and Z. Y. Li, "On-chip optical diode based on silicon photonic crystal heterojunctions," Opt. Express **19**, 26948–26955 (2011).
5. X. Wu and C. Fu, "Broadband and high-contrast-ratio optical diodes based on polarization conversion and photonic bandgap," J. Opt. **20**, 075603 (2018).
6. C. Ba, L. Huang, W. Liu, S. Li, Y. Ling, and H. Li, "Narrow-band and high-contrast asymmetric transmission based on metal-metal-metal asymmetric gratings," Opt. Express **27**, 25107–25118 (2019).
7. E. H. Turner and R. H. Stolen, "Fiber Faraday circulator or isolator," Opt. Lett. **6**, 322–323 (1981).
8. D. Jalas, A. Petrov, M. Eich, W. Freude, and H. Renner, "What is—and what is not—an optical isolator," Nat. Photonics **7**, 579–582 (2013).
9. R. Zhu, X. Wu, Y. Hou, G. Zheng, J. Zhu, and F. Gao, "Broadband asymmetric light transmission at metal/dielectric composite grating," Sci. Rep. **8**, 999 (2018).
10. L. Feng, M. Ayache, J. Huang, Y. L. Xu, M. H. Lu, Y. F. Chen, Y. Fainman, and A. Scherer, "Nonreciprocal light propagation in a silicon photonic circuit," Science **333**, 729–733 (2011).
11. L. Fan, J. Wang, L. T. Varghese, H. Shen, B. Niu, Y. Xuan, A. M. Weiner, and M. Qi, "An all-silicon passive optical diode," Science **335**, 447–450 (2012).
12. A. Ozer, H. Kocer, and H. Kurt, "Broadband and polarization-independent asymmetric transmission of visible light through a three-dimensional trapezoidal metallic metasurface," J. Opt. Soc. Am. B **35**, 2111–2117 (2018).
13. S. Cakmakyapan, H. Caglayan, A. E. Serebryannikov, and E. Ozbay, "Experimental validation of strong directional selectivity in nonsymmetric metallic gratings with a subwavelength slit," Appl. Phys. Lett. **98**, 051103 (2011).
14. Y. Ling, L. Huang, W. Hong, T. Liu, Y. Sun, J. Luan, and G. Yuan, "Asymmetric optical transmission based on unidirectional excitation of surface plasmon polaritons in gradient metasurface," Opt. Express **25**, 13648–13658 (2017).
15. D. Law, J. D'Ambroise, P. Kevrekidis, and D. Kip, "Asymmetric wave propagation through saturable nonlinear oligomers," Photonics **1**, 390–403 (2014).
16. V. A. Fedotov, P. L. Mladyonov, S. L. Prosvirnin, A. V. Rogacheva, Y. Chen, and N. I. Zheludev, "Asymmetric propagation of electromagnetic waves through a planar chiral structure," Phys. Rev. Lett. **97**, 167401 (2006).
17. M. Mutlu, A. E. Akosman, A. E. Serebryannikov, and E. Ozbay, "Asymmetric transmission of linearly polarized waves and polarization angle dependent wave rotation using a chiral metamaterial," Opt. Express **19**, 14290–14299 (2011).
18. C. Huang, Y. Feng, J. Zhao, Z. Wang, and T. Jiang, "Asymmetric electromagnetic wave transmission of linear polarization via polarization conversion through chiral metamaterial structures," Phys. Rev. B **85**, 195131 (2012).
19. O. Arteaga, B. M. Maoz, S. Nichols, G. Markovich, and B. Kahr, "Complete polarimetry on the asymmetric transmission through subwavelength hole arrays," Opt. Express **22**, 13719–13732 (2014).
20. T. Aba, Y. Qu, T. Wang, Y. Chen, H. Li, Y. Wang, Y. Bai, and Z. Zhang, "Tunable asymmetric transmission through tilted rectangular nanohole arrays in a square lattice," Opt. Express **26**, 1199–1205 (2018).
21. X. Li, W. Liu, and W. She, "Asymmetric optical transmission through silver film with a hyperbolic air hole," J. Opt. Soc. Am. B **35**, 886–891 (2018).
22. Z. Wu, J. Chen, M. Ji, Q. Huang, J. Xia, Y. Wu, and Y. Wang, "Optical nonreciprocal transmission in an asymmetric silicon photonic crystal structure," Appl. Phys. Lett. **107**, 221102 (2015).
23. H. Kurt, D. Yilmaz, A. E. Akosman, and E. Ozbay, "Asymmetric light propagation in chirped photonic crystal waveguides," Opt. Express **20**, 20635–20646 (2012).

24. C. Menzel, C. Helgert, C. Rockstuhl, E. B. Kley, A. Tunnermann, T. Pertsch, and F. Lederer, "Asymmetric transmission of linearly polarized light at optical metamaterials," Phys. Rev. Lett. **104**, 253902 (2010).
25. M. Kang, J. Chen, H. X. Cui, Y. Li, and H. T. Wang, "Asymmetric transmission for linearly polarized electromagnetic radiation," Opt. Express **19**, 8347–8356 (2011).
26. A. S. Schwanecke, V. A. Fedotov, V. V. Khardikov, S. L. Prosvirnin, Y. Chen, and N. I. Zheludev, "Nanostructured metal film with asymmetric optical transmission," Nano Lett. **8**, 2940–2943 (2008).
27. M. Stolarek, D. Yavorskiy, R. Kotynski, C. J. Zapata Rodriguez, J. Lusakowski, and T. Szoplik, "Asymmetric transmission of terahertz radiation through a double grating," Opt. Lett. **38**, 839–841 (2013).
28. B. Tang, Z. Li, Z. Liu, F. Callewaert, and K. Aydin, "Broadband asymmetric light transmission through tapered metallic gratings at visible frequencies," Sci. Rep. **6**, 39166 (2016).
29. J. Qiu and J. Xu, "Terahertz wave asymmetric transmission based on double-layer subwavelength dielectric grating," Opt. Eng. **58**, 067102 (2019).
30. H. Zhu, F. Li, B. Tang, X. Zang, and C. Jiang, "Asymmetric transmission through metallic grating with dielectric substrate," Opt. Commun. **318**, 41–46 (2014).
31. L. Zinkiewicz, J. Haberko, and P. Wasylczyk, "Highly asymmetric near infrared light transmission in an all-dielectric grating-on-mirror photonic structure," Opt. Express **23**, 4206–4211 (2015).
32. S.-T. Xu, F.-T. Hu, M. Chen, F. Fan, and S.-J. Chang, "Broadband terahertz polarization converter and asymmetric transmission based on coupled dielectric-metal grating," Ann. Phys. **529**, 1700151 (2017).
33. Y. Xie, H. Liu, H. Jia, and Y. Zhong, "Surface-mode model of the extraordinary optical transmission without plasmons," Opt. Express **23**, 5749–5762 (2015).
34. A. D. Rakic, A. B. Djurisic, J. M. Elazar, and M. L. Majewski, "Optical properties of metallic films for vertical-cavity optoelectronic devices," Appl. Opt. **37**, 5271–5283 (1998).
35. P. Lalanne and M. Hutley, "The optical properties of artificial media structured at a subwavelength scale," in *Encyclopedia of Optical Engineering* (2003), pp. 62–71.
36. G. Sridharan and S. Bhattacharya, "Simplified analysis of subwavelength triangular gratings by simplified modal method," Appl. Opt. **55**, 9712–9718 (2016).
37. I. H. Malitson, "Interspecimen comparison of the refractive index of fused silica," J. Opt. Soc. Am. **55**, 1205–1209 (1965).